Study on a Frequency-Stabilized Power-Adjustable Magnetron

Xiaojie Chen, Hang Lin, Zhenlong Liu, Kama Huang, Changjun Liu

School of Electronic and Information Engineering, Sichuan University, Chengdu 610064, China
cjliu@ieee.org

***Abstract*—A frequency-stabilized power-adjustable magnetron (FSPAM) has been theoretically analyzed by an equivalent model. It is found that numerical results were roughly conformed to the experimental performances of a practical injection-locked 20 kW magnetron. The frequency was shifting during power adjustment due to frequency pushing characteristic, and the locking condition will fluctuate instantaneously. This is the first time to introduce the metabolic data of frequency and power variation into the equivalent model to facilitate the prediction of its varied status. The proposed state equation were computed for the case of the power-variable magnetron with constant injected signal.**

Index Terms — frequency-stabilized, injection-locking, low interference, power dynamic scope

I. Introduction

Microwave absorption is dynamic change in microwave material processing, so power-adjustable magnetron is necessarily required to prevent materials burn or explosion [1]. Magnetron power-adjustment is easily realized by variations of anode voltage or anode current [2]. Unfortunately, central frequency of free-running magnetron will shift due to frequency pushing effect. Meanwhile, the devices of adjacent communication channel are vulnerably interfered by the wideband and noisy free-running power-variable magnetron.

It's attractive to obtain the power-adjustable magnetron with low interference. With regard to output improvement of a conventional magnetron, T. Mitani mentioned that the spectrum quality is greatly improved with filament-off [3] and Z. Liu had showed that the "Load-Pull mechanism" facilitate a low power-ratio injection-locked magnetron as an low-spurious amplifier [4]. N. Shinohara had achieved the 2.45 GHz injection-locked phase and amplitude controlled magnetron (PACM) by phase lock loop (PLL) [5], and B. Yang extended this work and delivered a 5.8 GHz PACM with a high response sensitivity in microsecond class [6].

In this paper, we developed an equivalent model to describe the output performance of injection-locked magnetron first. After verifying models' feasibility based on an industrial 20 kW CW magnetron experimentally, it's the first time coupled the "frequency pushing" data into formula to numerically investigate the real-time condition of this power-variable magnetron. It's aimed at theoretically exploring the power dynamic scope of the frequency-stabilized state.

II. The Equivalent Model

We shall first consider the magnetron with injected power as an admittance network [7], as shown in Fig. 1. The microwave (MW) power is generated by electron interactions which is represented by $-(g+jb)$, anode cavity can be equivalent by parallel RLC circuit. The external load is described by $G+jB$. An injected reference signals' current I_1 and voltage V_1 is applied to lock the magnetron and can be regarded as $G'+jB'$.

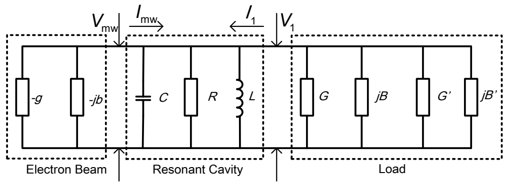

Fig. 1. The equivalent model based on admittance network.

Volt-ampere energy conversion of the model in Fig. 1 can be written as:

$$-(g+jb)V_{mw}=\frac{V_{mw}}{R}+\frac{V_{mw}}{j\omega L}+j\omega CV_{mw}+C\omega_0\frac{(G+jB)+2|\rho|e^{j\theta}}{Q_{ext}}V_{mw} \quad (1)$$

V_{mw} is output MW voltage of magnetron, which has fast temporal component of $e^{j\omega t}$ so that $V_{mw}=V_{mw}(t)\cos(\omega t)$, where $V_{mw}(t)$ is slowly varying in time, Q_{ext} is the external quality factor and ω_0 can be expressed by $\sqrt{LC}$. Injection ratio ρ is equal to $\sqrt{P_1/P_0}$ and θ means the phase difference between magnetron self-oscillated signal and reference signal, then V_{mw} is updated to the form $V_{mw}=V_{mw}(t)\cos(\omega t)$. Formula (1) is able to be decoupled into two normalized time domain differential equations that they are valid to analyze the phase difference and MW voltage of magnetron, where all the frequencies are normalized by ω_0:

$$\frac{d\theta}{dt}+1-\omega_1=\frac{\rho}{Q_{ext}}\sin\theta \quad (2)$$

$$\frac{1}{V_{mw}}\frac{dV_{mw}}{dt}+\frac{1}{Q_0}\left(1-\frac{1}{V_{mw}}\right)=-\frac{\rho}{Q_{ext}}\cos\theta \quad (3)$$

The equation (3) contains θ, only simultaneous solution method can obtain V_{mw} and then get the spectrum. Additionally, $d\theta/dt$ equals to zero when magnetron is fully synchronized with reference signal, a new form we get is well-known Adler equation [8]:

$$|1-\omega_1|=\rho/2Q_{ext} \quad (4)$$

Equations (2) and (3) were solved by Runge-Kutta method [9], the Fast Fourier Transform (FFT) was used to calculate the V_{mw} , where sample frequency is f_s=4 Hz. Fig. 2 exhibited the numerical calculation of spectra of magnetron with different injected condition. The parameter setup: injected frequency ω_1=0.998 Hz, Δf=0.002, $\rho/2Q_{ext}$ is equal to 0.00195 and 0.0025, respectively.

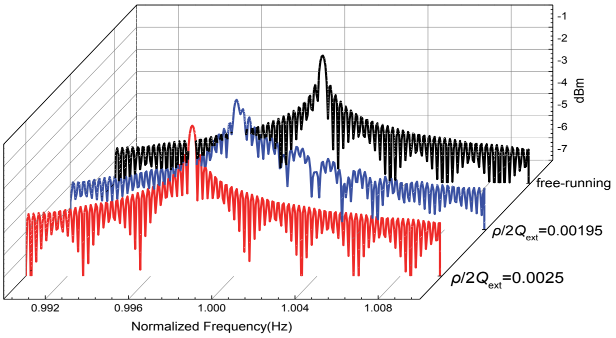

Fig. 2. Numerical results of different injected condition.

The blue solid line presents a phenomena that the strong and spurious sideband is opposite the injected frequency, which is caused by AM/FM of beat. The totally synchronized spectrum is presented by the red solid line, the output frequency of magnetron is migrated to 0.998 Hz from origin condition (black solid line). It's worth mentioning that decrement of Δf is equivalent to $\rho/2Q_{ext}$ increment.

III. Experiments Results

We had conduct an experiment based on an S-band 20 kW CW magnetron named CK-2091 which manufactured by Nanjing Sanle Information Industry Group. Company Ltd. Fig. 3 shows the practical magnetron and measurement system block diagram, where output power and spectrum were monitored by power meter (AV2433, the 41st Institute of CETC) and spectrum analyzer (FSV40, Rohde & Schwarz), respectively.

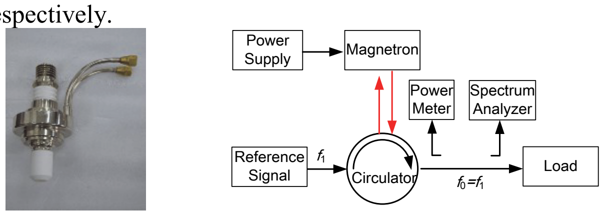

(a) (b)

Fig. 3. (a) Water-cooled CK-2091 magnetron. (b) Injection-locked magnetron diagram.

As we can see in Fig. 4, free-running magnetron with 18.0 kW output power was oscillating in a certain bandwidth (about 1.2 MHz) which central frequency is 2.4498 GHz. Then a 2.4478 GHz, 100.0 W reference signal injected into magnetron, the stray sideband was aroused just like what we had discussed in Sec. II. Besides, the spurious sideband which might interfere the communication devices at the criterion of IEEE 802.11 b, g, such as Wi-Fi system or Zig-bee sensor.

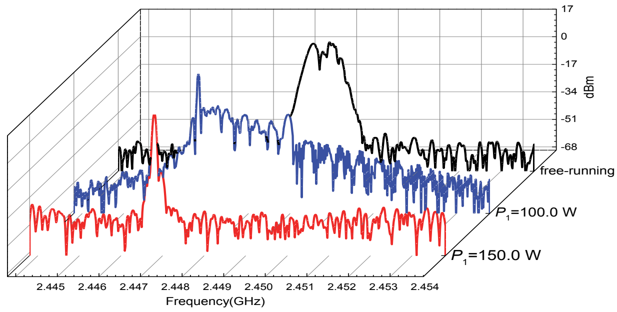

Fig. 4. Experimental results of different injection ratio.

The magnetron delivered a sharp spectrum while the injected power was rising to 150.0 W. The spurious noise was suppressed and the magnetron was stably locked at 2.4478 GHz, the peak value of locked spectrum was over 1 dB higher than others due to energy concentration.

TABLE.I
MEASUREMENT RESULTS

I_a(A)	0.70	1.00	1.44	1.88	2.30
f_0(GHz)	2.442	2.445	2.449	2.450	2.450
P_o(kW)	5.74	8.69	11.62	15.20	18.90

Draw back to our previous works, we had investigated the "frequency pushing" characteristics of free-running CK-2091 by anode current I_a variation [10], the detail data was shown in Table. I. Apparently, the data illustrated that magnetron is suitable to power-control but the frequency drift may cause unexpected interferences in industry applications.

IV. Updated Equivalent Model and Calculations

In order to clearly study the power scope at frequency-stabilized condition, we considered the I_a of CK-2091 was temporal and linearly increased, so that the variation of ω_0 and P_o had a one to one mapping relationship with I_a, respectively. We set P_{nor}=11.02 kW as a reference power point when magnetron is working at I_a=1.4 A, f_{nor}=2.4491 GHz, and $\omega_0(I_a)$ and $P_o(I_a)$ are normalized, respectively. Then we introduced $\omega_0(I_a)$ and $P_o(I_a)$ into equation (3) and assumed that the fixed frequency of injected signal was f_1=f_{nor}, then we obtained:

$$\frac{d\theta}{dI_a} + \omega_{nor}(I_a) - 1 = \frac{\omega_{nor}(I_a)\times\rho_{non}\sqrt{1/P_{nor}(I_a)}}{2Q_{ext}}\sin\theta \qquad (5)$$

$$\omega_o(I_a) = \omega_{1nor} - \frac{d\theta}{dI_a} \qquad (6)$$

where power ratio is to be $\rho_{non} = \sqrt{P_1/P_{ref}} \times \sqrt{1/P_{nor}(I_a)}$, which seems to be nonlinear, the same as frequency difference $\Delta f_{non} = |f_0 - f_{nor}(I_a)|$ when the external Q value isn't varied by power adjustment. We assumed the fixed injection power are 50.0 W, 100.0 W and 200.0 W.

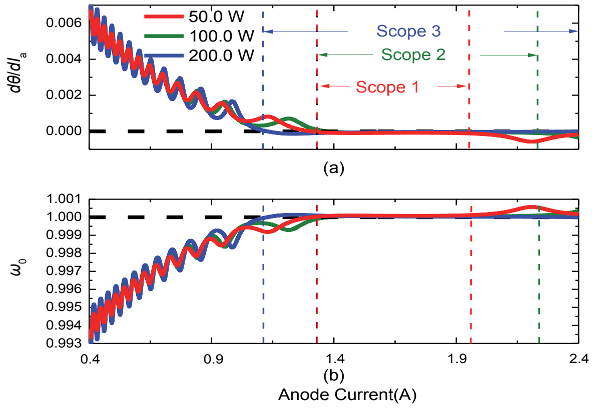

Fig. 5. Frequency variation at power adjustment with fixed injection.

Fig. 5 exhibited the numerical results of anode current domain frequency and differential phase. The results could roughly predict injection-locking to occur when the $d\theta/dI_a$ becomes constant and extremely close to zero (Fig. 5 (a), scope 1 to 3). Within those scopes, the Adler's condition is satisfied and we expected the output frequency to track the injected frequency, where $\omega_o(I_a)=\omega_1-d\theta/dI_a$. $\omega_o(I_a)$ is approximately regarded as ω_1, with extremely small $d\theta/dI_a$ (Fig. 5 (b)). Since the magnetron performs outside the scope, both $d\theta/dI_a$ and $\omega_o(I_a)$ oscillate at a beat Δf_{non}. Fig 5 also demonstrates that the wider frequency-stabilized power-adjustable scope is brought by higher injected power. At theoretical condition, Scope 3 represents frequency-stabilized power dynamic scope which starts from 8.7 kW to 19.7 kW, the corresponding anode current varies from 1.1 A to 2.4 A.

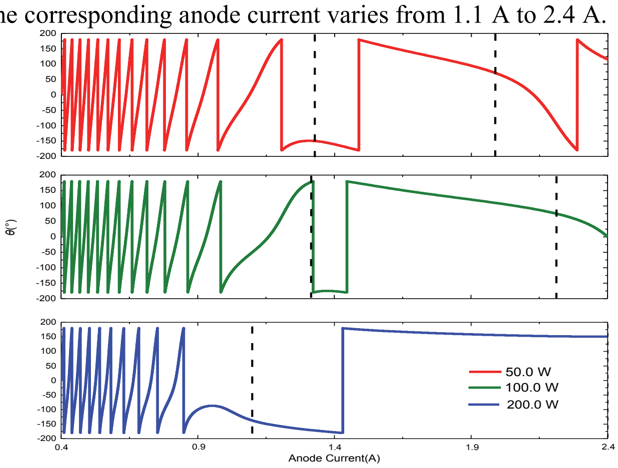

Fig. 6. Phase variation at power adjustment with fixed injection.

The insufficient synchronized condition leads to violently fluctuation of phase difference when the anode current is initially outside the locking scope, as shown in Fig. 6. Once current gradually closed to locking scope (shown in Fig. 5), the phase difference value will be constant when $d\theta/dI_a$ approach zero. In the locking scope, the alteration of phase difference is just relevant to the nonlinear variation of beat Δf, injection condition ρ/Q_{ext}. Moreover, the range of phase alteration were compressed by higher injected power at fixed frequency, the theoretical results showed that the steady phase-varied range of 200.0 W injection (about 71°) is nearly half of the 50.0 W injection (about 135°).

V. Conclusion

The equivalent model of FSPAM is studied. The viability of equivalent model is verified by an S-band 20 kW CW magnetron with injected power. The model was coupled with practical "frequency pushing" data which was used to predict power-adjustable scope at constant frequency. We had theoretically obtained a pretty wide frequency-stabilized power dynamic scope of 11.0 kW with fixed injection (200.0 W at 2.4491 GHz). Moreover, phase difference compression effect was numerically found at the higher injected-power condition. Therefore, the proposed model is to some extent appropriate to indicate that FSPAM is expected to work as a low-spurious level and wide power dynamic scope microwave source in industrial applications.

Acknowledgement

The work was supported in part by 973 program 2013CB328902.

References

[1] B. Lin, H. Li, H. Dai, C. Zhu, and H. Yao, "Three-dimensional simulation of microwave heating coal sample with varying param-eters," Appl. Therm. Eng., vol. 93, pp. 1145–1154, 2016.
[2] A Gilmour. Klystrons, traveling wave tubes, magnetrons, crossed-field amplifiers, and gyrotrons[M]. Artech House, 2011.
[3] T Mitani, N Shinohara, H Matsumoto, et al. Experimental research on noise reduction of magnetrons for solar power station/satellite[C]//Radio Science Conference, 2004. Proceedings. 2004 Asia-Pacific. IEEE, 2004: 603-606.
[4] Z Liu, X Chen, M Yang, et al. Experimental Studies on a 1-kW High-Gain S-Band Magnetron Amplifier With Output Phase Control Based on Load–Pull Characterization[J]. IEEE Transactions on Plasma Science, 2018, 46(4): 909-916.
[5] N Shinohara, H Matsumoto. Microwave power transmission system with phase and amplitude controlled magnetrons [C]//Recent Advances in Space Technologies, 2005. RAST 2005. Proceedings of 2nd International Conference on. IEEE, 2005: 28-33.
[6] B Yang, T Mitani, N Shinohara. Experimental Study on a 5.8 GHz Power-Variable Phase-Controlled Magnetron[J]. IEICE Transactions on Electronics, 2017, 100(10): 901-907.
[7] J Slater. The phasing of magnetrons[J]. 1947.
[8] R. Adler, "A study of locking phenomena in oscillators," Proc. IEEE, vol. 61, no. 10, pp. 1380–1385, 1973.
[9] P Pengvanich, Y Lau, J Luginsland, et al. Effects of frequency chirp on magnetron injection locking[J]. Physics of Plasmas, 2008, 15(7): 073110.
[10] X. Chen, H. Huang, W. Jiang, and C. Liu, "Study on microwave coherent power combining based on 20-kW S-band CW power-adjustable magnetrons," J. Electromagn. Waves Appl., vol. 31, no. 17, pp. 1835–1842, 2017.